Time-Frequency Dynamics of Resting State Effective Connectivity in the Default Mode Network

Gopikrishna Deshpande[1,2], Hao Jia[1], Zhihao Li[3], and Xiaoping Hu[3]

[1]AU MRI research center, Dept. of ECE, Auburn University, Auburn, Alabama, United States, [2]Dept. of Psychology, Auburn University, Auburn, Alabama, United States, [3]Coulter Dept of Biomedical Engineering, Georgia Institute of Technology and Emory University, Atlanta, Georgia, United States

Introduction

A recent report indicates that functional connectivity in resting state networks show dynamic patterns in time and frequency [1]. Although theneurophysiological origin of frequency-specific non-stationary nature of instantaneous correlation between resting state BOLD time series is yet unclear, this phenomenonhas evoked a great deal of interest in the fMRI community. In this work, we hypothesized that effective connectivity between resting state fMRI time series also dynamically evolve across time and frequency. We tested this hypothesis by calculating dynamic Granger causality between the core areas of the resting state network.

Methods

Resting state EPI data were obtained from 26 healthy volunteers(13 male, 13 female with age 15.1 ± 1.1 years) using a Siemens 3T scanner with standard EPI sequence and the following parameters: 210 time points, matrix=64×64, 20 axial slices without gap, slice thickness=4 mm, TR/TE=2000 ms/30 ms, flip angle=90°, FOV =192 cm, and a total scan time of 7 minutes for each subject. Standard pre-processing includes: slice-timing correction, rigid body registration, 0.01 Hz < f < 0.1 Hz band-pass filtering and 5 mm full width half max Gaussian smoothing.Resting state networks included 4 networks: Default mode network (DMN), hippocampal cortical memory network (HCMN), dorsal attention network (DAN) and fronto-parietal control network (FPCN) identified from published co-ordinates [2, 3,4].Mean time series corresponding to 33 ROIs from the above networks were obtained from 2 cm^3 non-overlapping spheres around the hotspotsand decomposed into 120 wavelet scales in the frequency range of 0.01 to 0.1 Hz, using the complex Morlet wavelet with center frequency ω=6.This has been shown to provide an approximately linear correspondence between scale and frequency [1]. The time series at each scale was then input into an adaptive multivariate autoregressive model and its coefficients estimated using the Kalman filter algorithm. The model order for each scale was determined using the Bayesian information criterion. For the given model order and scale, the forgetting factor for the Kalman filter was determined based on minimum error variance obtained from the model [5]. The Kalman filter structure was updated with time series data from every subject such that the coefficients obtained by using data from all the 26 subjects represented group-level metrics. The 33 × 33 connectivity matrix at each time point and scale represented a feature vector which was initially clustered in time using k-means clustering. And then, we usedthe k-means cluster centroids as reference points, and quantization was performed in time using the neural gas algorithm such that connectivity patterns across the entire network, which were similar, were agglomerated in time. The number of centroids *k*represents the number of finite states that the connectivity matrix can assume, andthe choice of this number was madeusing an iterative procedure as follows.By executing Eigen decomposition of geodesic distance matrixof the high dimensional manifold which consisted of connectivity matrices at all time points,we checked if we can eliminate anyEigen value, while retaining more than 95% of the original total energy, and if yes, *k*was reduced by 1. This procedure was iterated until *k*could be reduced further.

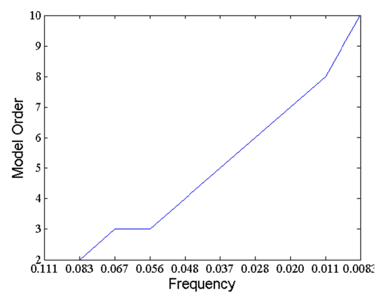

Figure 1: Model order as a function of frequency

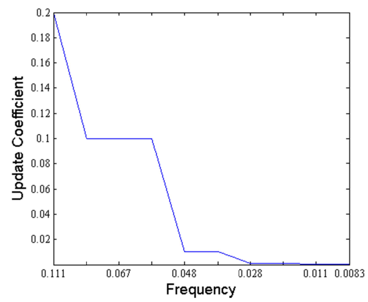

Figure 2: Update coefficient as a function of frequency

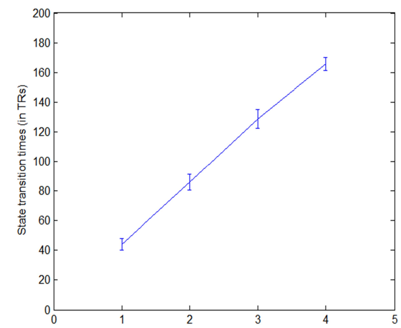

Figure 3: State transition times

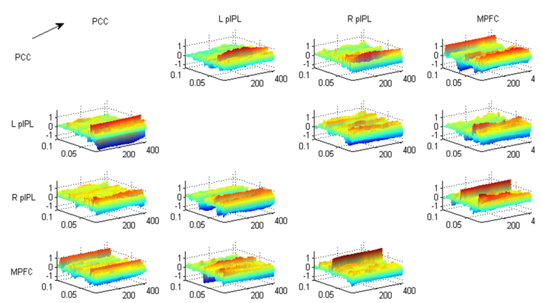

Figure 4: Time-frequency dynamics of default mode effective connectivity. Rows represent outputs and columns represent inputs. In each sub-plot, x, y and z axes represent time in seconds, frequency in Hz and effective connectivity strength, respectively.

Results and discussion

Fig.1 shows that model order increases and update coefficient of the Kalman filter decreases with decreasing frequency. It indicates that for lower frequencies, the model remembers longer into the past. This makes sense because in order to capture slow variations, the model needs to have longer memory.We found that the connectivity pattern of the entire network agglomerated into 5 distinct states, i.e. resting state effective connectivity toggled between 5 states during the 7 minute scan for all the frequencies. Fig.3 shows the mean and standard deviation of the times during which a state transition occurred across all frequencies. It can be seen that a state lasts 40-45 TRs or 80-90 seconds. The time-frequency dynamics of effective connectivity, given by the variation of the model coefficients with time and scale, of the core regions of the DMN is shown in Fig.4. It can be seen that different paths have different dominant frequencies. In addition, causality at certain scales remains relatively constant with time while those at others display non-stationarity. These results confirm our hypothesis that not only functional, but also effective connectivity in resting state networks dynamically change with time and frequency. In addition, the existence of a finite number states across time represents a new finding of the resting state. Further investigation is required in order to understand the neurophysiological significance of these observations.

Conclusion

We have revealedthat effective connectivity assumes a finite number, e.g. 5 as in here, of states during rest. Also, the time-frequency dynamics of effective connectivity in the default model network has frequency-specific signatures which could consist of both stationary and non-stationary components.For further development, studies using longer data are required to confirm this observation and the neurophysiological significance of this limited non-stationarity needs to be explored.

References

1. Chang C., et al, NeuroImage, 50(1): 81-98, 2010. **2**.Grecius M., et al, Proceedings of the National Academy of Sciences USA, 100: 253-258, 2003. **3**. Grecius M, et al. PNAS 100: 253-258, 2003.**4**. Vincent, et al. J Neurophys 100: 3328-3342, 2008.**5**. Schlogl A., et al, In: IEEE (Ed.), Proceedings of the 22nd IEEE International Conference on Engineering in Medicine and Biology, pp. 1581–1582, 2000.